HIGH PERFORMANCE VOLTAGE CONTROL USING FEEDBACK LINEARIZATION

Jeffrey D. Lindlau
Motorola Automotive and Industrial Electronics Group, Northbrook, IL , USA, ***
Carl R. Knospe
Department of Mechanical and Aerospace Engineering, University of Virginia, Charlottesville, Virginia, USA, crk4y@virginia.edu

ABSTRACT
In this paper, a feedback linearization controller is presented for a single DOF magnetic bearing test rig. The feedback linearization controller is derived from a detailed nonlinear electromagnet model using both analytic relationships and experimental calibration data. A high performance controller for the feedback linearized plant is designed with μ-synthesis to guarantee a beam compliance performance specification. Experimental results demonstrate that the μ controller with feedback linearization achieves the performance specified during design for the nonlinear plant independent of the disturbance force level or displacement incurred.

INTRODUCTION
Active magnetic bearings (AMBs) are increasingly used in industrial rotating machinery applications. Often, a linear model of these actuators is used to approximate the nonlinear relationship between force, current, and air gap length thus providing a model suitable for the design of linear controllers. A disadvantage to this approach is that the linear model is approximated at a single operating point, and the validity of this model decreases as the physical system is perturbed from this point. Accommodating this degradation typically results in increased conservatism in both the actuator and control system design, reducing the AMB's performance. In this paper we consider feedback linearization to reduce the nonlinear AMB model to a linear plant that is valid for all operating points and suitable for modern linear controller design. This approach has been previously considered for AMB systems [1,2]. However, in these efforts the bearing models are analytically based and do not consider AMB non-idealities such as flux saturation and leakage, which are functions of both current and air gap.

In this paper, feedback linearization controllers are examined for a one degree of freedom magnetic suspension and implemented in voltage control mode. Since the effectiveness of a feedback linearization controller is a reflection upon the accuracy of the nonlinear model used in its derivation, strong emphasis is placed on the development of a detailed nonlinear electromagnet dynamic model. A second goal of this paper is to demonstrate that a high performance model-based controller designed for the feedback linearized AMB will achieve a specified performance regardless of variation in operating point.

ONE DEGREE OF FREEDOM TEST RIG
The one DOF test rig pictured in Figure 1, consists of two actuators and a symmetric steel beam resting atop a pivot. The beam is imbalanced by the addition of an aluminum mass to one end and the beam angle is stabilized by control of the electromagnet at the opposite end. The second electromagnet is only used to apply a disturbance force to the system. This test rig is easily modeled from a mechanical viewpoint, yet still encompasses all the nonlinear characteristics inherent to a typical AMB system.
Two PWM power amplifiers were used in voltage mode to drive the electromagnets. An eddy current type displacement sensor provides measurement of the gap length and beam angle, while an LEM LA 50-P sensor provides measurement of the coil current. Lastly, 16 bit A/D and D/A boards are used with a dSPACE DS1004 digital controller for real time feedback algorithm execution, model simulation, and data acquisition. Table 1 details some of the physical characteristics associated with the test rig.

TABLE 1: Test Rig Physical Characteristics

Physical Quantities	Value
Beam Length	0.32 m (12.6 in.)
Beam Mass	9.93 kg (21.89 lb.)
l, length from pivot to actuator centerline	0.145415 m (5.725 in.)
r, length from pivot to center of mass	0.01 m (0.394 in.)
J, Beam Polar Moment of Inertia	0.0967 kg-m^2 (.071 slug-ft^2)
Nominal (centered) gap	0.3302 mm (13 mils)
Maximum Gap (beam at one auxiliary stop)	0.5842 mm (23 mils)
Minimum Gap (beam at other auxiliary stop)	0.0762 mm (3 mils)
N, number of coil turns	321
R, Coil Resistance	1.6 Ω
A_{gap} (pole face area)	101.69 mm^2 (0.1576 in.^{2})
Peak Force (at centered position)	85 N (19.1 lbf)

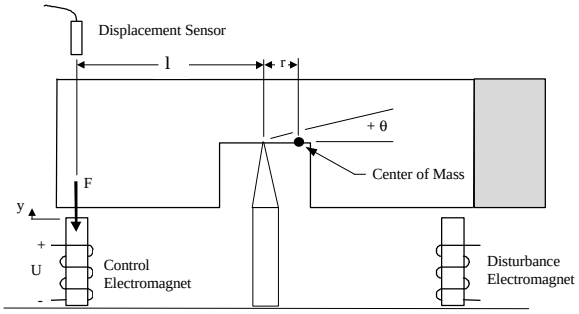

FIGURE 1: One DOF Beam Balancing Test Rig

SYSTEM MODELING OVERVIEW

The system model consists of a mechanical model describing the beam motion coupled with a dynamic electromagnetic actuator model. By ignoring the beam's flexible mode dynamics (which we will return to later), the equation of motion for the unbalanced beam may be written by summing the applied moments about the pivot:

$$J\ddot{\theta} = lF - Mgr \qquad (1)$$

where M is the mass of the unbalanced beam, g is the gravitational constant, l is the distance from the center of the electromagnet pole face to the pivot, r is the displacement of the center of mass to the pivot, and J is the beam's polar moment of inertia. This equation is analogous to the model for the gravity biased magnetic suspension of a steel ball examined in [4].

The force generated by the electromagnet can be modeled by the nonlinear relationship

$$F = k\phi_g^{\,2} \qquad (2)$$

where ϕ_g refers to the magnetic gap flux and k is a constant dependent upon actuator geometry. In turn, the gap flux ϕ_g is a nonlinear function of the *total* magnetic flux ϕ and the air gap length as described below:

$$f_g = f(f, y) \qquad (3)$$

(This flux leakage function will be examined in greater detail in the next section.) The electromagnet's dynamic model is governed by the following equation:

$$N\dot{\phi} = U - iR \qquad (4)$$

where N is the number of coil turns, $\dot{\phi}$ is the time derivative of the total flux linked by the coil turns, U is the voltage supplied across the coils, i is the current flowing through the coils, and R is the coil's electrical resistance.

ELECTROMAGNETIC ACTUATOR MODELING

Static Force Calibration.

From standard linear magnetic circuit analysis, the relationship between gap flux and current for the actuator's EI shaped geometry is:

$$\phi_g = \frac{2Ni\mu_o A_{gap}}{(3y + l_{equiv})} \qquad (5)$$

The total force produced by the electromagnet is (see [5] for a detailed derivation):

$$F = \frac{3\phi_g^{\,2}}{4\mu_O A_{gap}} \qquad (6)$$

Note that flux saturation in the actuator is not considered in equation 5, however equation 6 is accurate even in this case unless the flux saturation is quite severe. To eliminate the use of a flux sensor, an extensive static calibration of the electromagnet was performed in order to develop a calibration table for online flux estimation (see [5]) shown in Figure 2.

Leakage Flux Effects

While the flux calibration table may be used to estimate the gap flux from available current and beam position measurements, the AMB's electrodynamics are in terms of total flux as indicated in equation 4. The relationship between these two variables is defined by the flux leakage function introduced in equation 3. To determine this function, the authors employed the

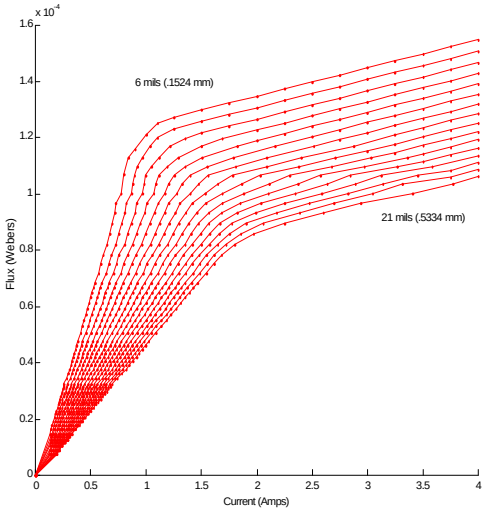

FIGURE 2: Flux Calibration Table

magnetic finite element code FEMM[1] to analyze the electromagnets on the experimental test rig. A series of finite element analyses indicate the ratio of the gap flux to the total flux to be nearly independent of the current level (less than 5% variation), but to vary significantly with air gap length. The data indicates that a satisfactory leakage function model (recall equation 3) is:

$$\phi_g = f(\phi, y) = p_1(y)\phi \tag{7}$$

where

$$p_1 = \frac{1}{ay + b} \tag{8}$$

and a and b are constants determined from the fit.

Dynamic Model

Figure 3 shows a block diagram of the electromagnet dynamic model combining equation 2, equation 4 and the leakage flux term, p_1. This electromagnet dynamic model will be used for controller development. It is a nonlinear model that accounts for magnetic material saturation, leakage flux, and hysteresis (since the model is in terms of flux and current is an input). Other common non-idealities such as gap dependent flux fringing and eddy currents effects are not considered in this model. From the authors' experience, these effects are not particularly important in this experiment.

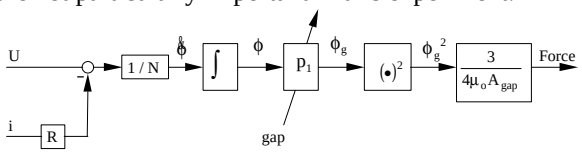

FIGURE 3: Electromagnet Dynamic Model Incorporating Leakage Flux

FEEDBACK LINEARIZATION CONTROLLER DEVIATION

A feedback linearization controller was designed for the nonlinear model (Figure 3) in order to produce a linear plant valid across the entire operating range. From equation (6) and (7) we have

$$\ddot{F} = 2cp_1^2\phi\dot{\phi} + 2c\phi^2 p_1\dot{p}_1 \tag{9}$$

Substitution of the analytical fit for p_1 (equation 8) and its derivative results in:

$$\ddot{F} = 2cp_1^2\phi\dot{\phi} - 2c\phi^2 p_1^3 a\dot{y} \tag{10}$$

Combining equations 4 and 10 yields:

$$\ddot{F} = \frac{2cp_1}{N}\sqrt{\frac{F}{c}}(U - iR) - 2Fp_1 a\dot{y} \tag{11}$$

and from (1)

$$\dddot{y} = \frac{2lcp_1}{N}\sqrt{\frac{F}{c}}(U - iR) - 2lFp_1 a\dot{y} \tag{12}$$

The control input voltage U can be chosen in the following manner:

$$U = U_{FL} = \frac{JN}{2lcp_1\sqrt{\frac{F}{c}}}V_{FL} + iR + \frac{NFa\dot{y}}{c\sqrt{\frac{F}{c}}} \tag{13}$$

to reduce the nonlinear system equation to the simple triple integrator linear plant:

$$\dddot{y} = V_{FL} \tag{14}$$

V_{FL} is the "new" control input to be provided by a linear feedback controller (yet to be designed).

FEEDBACK LINEARIZATION VALIDATION

A comparison of the theoretical feedback linearized system (a triple integrator plant) to an experimental transfer function of the open loop linearized plant presents a straightforward and convincing measure of the effectiveness of the feedback linearization controller. Figure 4 compares magnitude and phase plots of the experimental transfer function to that of the desired triple integrator plant. The experimental transfer function was obtained using the sine sweep mode of a HP 3566A Spectrum Analyzer. As seen in Figure 4, the experimental transfer function fails to match the theoretical linearized plant below 10 Hz and above 200 Hz. The mismatch above 200 Hz is caused by omission of the beam dynamics in the derivation of the feedback linearized plant. The discrepancy below 10 Hz was not originally anticipated. Further investigation indicated that this was due to uncertainty in the coil resistance.

[1]FEMM V2.0β1, provided by Dr. David Meeker, http://members.aol.com/dcm3c

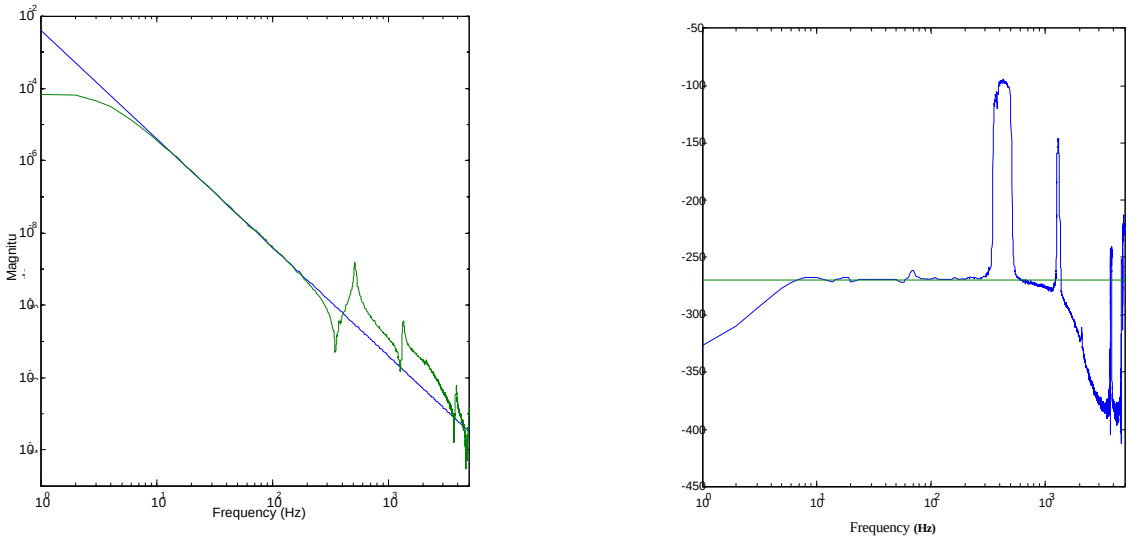

FIGURE 4: Open Loop Transfer Function of Feedback Linearized System, Theory (Triple Integrator) and Experiment

Incorporated of the Beam Dynamics into the Feedback Linearized Plant

The beam dynamics can be modeled as a linear transfer function, and simply connected in series with the theoretical linearized system to produce a new feedback linearized plant model:

$$\frac{\theta(s)}{V_{FL}(s)} = \frac{1}{s^3}\frac{n(s)}{d(s)} \qquad (15)$$

with n(s) and d(s) representing the numerator and denominator of the normalized transfer function for the beam dynamics. This transfer function was obtained by fitting the frequency response data presented in Figure 4 with a 4th order model capturing the first two modes.

Low Frequency Error-Coil Resistance Uncertainty

An investigation of the low frequency discrepancy between the measured and theoretical transfer functions found that the feedback linearization controller is extremely sensitive to coil resistance in the low frequency. Changing R from 1.45 Ω to 1.60 Ω causes the feedback linearized plant's magnitude at 1 Hz to change by a factor of five, and the phase to change by nearly 100 degrees. Thus, a small mismatch between the actual value of resistance and that assumed in the feedback linearization can produce a large discrepancy between the low frequency response of the theoretical plant model, and that actually obtained by the feedback linearized controller.

HIGH PERFORMANCE CONTROLLER DESIGN FOR THE FEEDBACK LINEARIZED PLANT

In this section, the design and application of a high performance model-based controller to the feedback linearized plant is described. This controller will be designed via μ-synthesis. [3,4]

Coil Resistance Uncertainty

To represent coil resistance uncertainty within the feedback linearized model, we consider the effect a mismatch in resistance has upon the electromagnet dynamics. Consider again equation for the electromagnet dynamics:

$$N\dot{\phi} = U - iR \qquad (16)$$

From the magnetic circuit derivations for the EI shaped electromagnet, it is possible to approximately represent the current as a function of flux (when saturation is ignored):

$$i = \gamma\phi \quad \text{where} \quad \gamma = \frac{3y + l_{equiv}}{2N\mu_o A_{gap}} \qquad (17)$$

This allows equation 16 to be represented in a feedback configuration: The feedback linearization control law, equation 13, indicates the direct cancellation of the product of current and resistance. By defining R^* to be the estimate of the actual resistance R, cancellation of this term in equation 13 can be represented by an additional feedback loop:

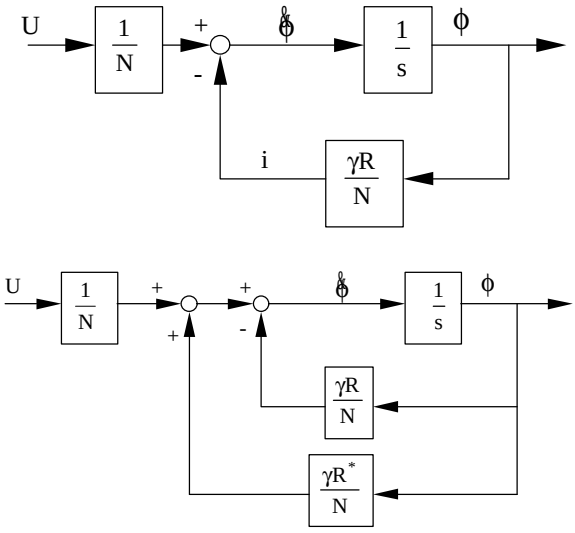

Thus the mismatch can be represented as an integrator with a feedback

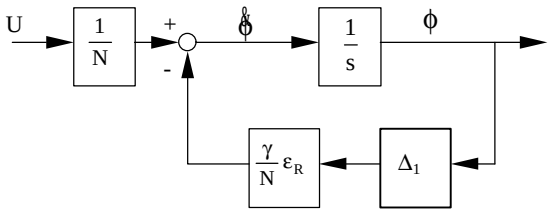

where ε_R is an estimate of the maximum error in the resistance estimate and Δ_1 is a unit norm (real) uncertainty. Based upon experience, a good value for ε_R is 0.05 Ω (R was measured as 1.6Ω at room temperature). Substituting N = 321 turns, and γ = 13749 H^{-1} evaluated at the centered position (y = 13 mils; 0.33 mm) the uncertainty weight is:

$$W_R = \frac{\gamma}{N}\varepsilon_R = 2.1$$

Performance Goals: Beam Compliance and Control Effort.

Two performance weights, W_d and W_c, associated with beam compliance (alternatively, actuator stiffness) and control effort, were also added to the nominal linearized plant model. The weighting on maximum control effort was chosen as follows:

$$W_c = \frac{(s+9000)^2}{2500(s+90000)^2} \qquad (18)$$

This specifies that at each frequency the feedback controller must have a gain less than $\left\|W_c(j\omega)^{-1}\right\|$. The filter restricts the control bandwidth to approximately 1400 Hz. (This filter choice was based upon the authors'

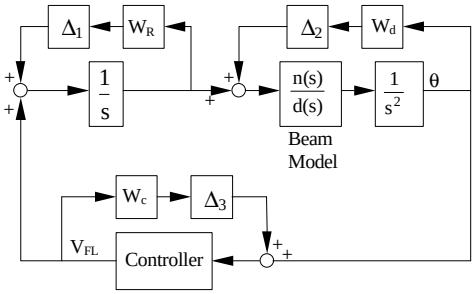

FIGURE 5: Nominal Linearized Plant with Uncertainty and Performance Weights

previous experience in designing controllers for this test rig.) The beam compliance weighting function, W_d was chosen as follows:

$$W_d = \frac{.03(s+500000)}{s+5000} \qquad (19)$$

and represents a maximum dynamic compliance specification of ≈ .33 mils/Lbf (.0017 mm/N) or a minimum dynamic stiffness specification for the bearing of 3400 Lbf/in. (5.95×10^5 N/m) from 0 to 600 Hz. This specifies that at each frequency the beam's compliance must have a gain less than $\left\|W_d(j\omega)^{-1}\right\|$. This weighting filter was determined from implementing μ-synthesis within a bisection search so as to increase its DC gain until μ ≈ 1. This procedure reduces the worst case (due to uncertainty) beam compliance over a frequency range inclusive of the first flexible beam mode. The μ controller was designed for the model represented in Figure 5 with the MATLAB μ toolbox. Each Δ block was represented as a complex, scalar LTI uncertainty even though Δ_1 is, in fact, real valued. The resulting controller was 22nd order, and achieved complex μ = 0.89. Using a standard balanced-truncation model reduction routine, this controller was reduced to 10th order and achieved a complex μ = 0.91, a slight degradation from the original value. The designed controller gain stabilizes the beam flexible mode at 520 Hz.

CONTROL EXPERIMENTAL RESULTS

The 10th order μ controller was successfully implemented in combination with the feedback linearization controller at 10Khz on the dSPACE DS1004 control platform. To show that the desired performance specification for beam compliance is satisfied, the right actuator (not employed by the feedback controller) was used as a disturbance source. By combining a similar feedback linearization controller derived for this electromagnet with its respective flux calibration table, the right actuator performed as a calibrated external force disturbance with negligible associated negative actuator stiffness, K_x. A HP3566A Spectrum Analyzer was used to excite the right actuator with a sine sweep signal added to a constant disturbance bias force, and a transfer function was measured from the

TABLE 2: Block Descriptions for LFT Model

Δ Block	Representation
Δ_1	Resistance (R) Uncertainty
Δ_2	Beam Compliance Performance Block
Δ_3	Control Effort Performance Block

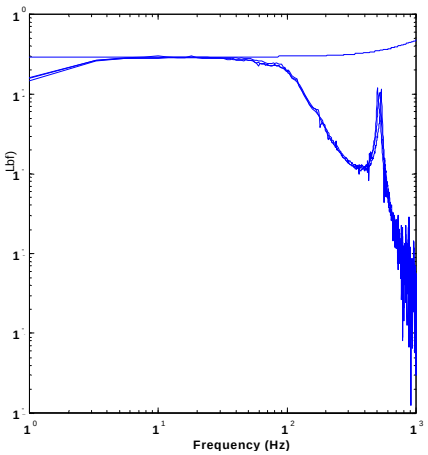

FIGURE 6: Experimental Frequency Response at Three Disturbance Bias Levels and Performance Specifications W_d^{-1}

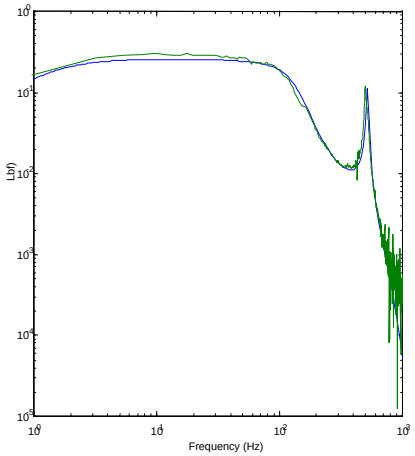

FIGURE 7: Compliance Frequency Responses for Experiment and Theoretical Model

disturbance force to the beam displacement. The bias disturbance forces cause the control (left) actuator to operate at different points along its magnetization curve. The results are shown in Figure 6 with measured compliance transfer functions plotted against the performance specification W_d^{-1}. In order to demonstrate that the μ performance specifications are valid across different operating points, three measured transfer functions are shown in the figure, indicating the frequency response with disturbance force biases of 10 N (2.24 Lbf), 22 N (4.95 Lbf), and 36 N (8.1 Lbf). The performance requirement is satisfied regardless of this disturbance force level and is largely invariant to it. In Figure 7, the experiment's frequency response to the disturbance force is compared to that of the theoretical model. The match between these responses is excellent.

CONCLUSION

In this paper, a feedback linearization controller is applied to a one DOF active magnetic bearing test rig with voltage control. A detailed nonlinear model was developed using both analytic relationships and experimental data. Experimental results confirm an excellent match between the theoretical and measured open loop feedback linearized system. Also, the nonlinear dynamic model was shown to be valid across large gap and current variations. A μ controller was then designed for the feedback linearized system to minimize a beam compliance performance specification. The issue of coil resistance variation is tackled by the inclusion of an uncertainty into the feedback linearized plant. Experimental results confirm that the μ performance specifications are satisfied, regardless of operating point.

REFERENCES

1 Trumper, D., Olson, S., Subrahmanyan, P., "Linearizing Control of Magnetic Suspension Systems", IEEE Transactions on Control Systems Technology, Vol.. 5, No. 4, pp. 427-437, July 1997.

2 Torres, M. and R. Ortega, "Feedback Linearization, Integrator Backstepping and Passivity-Based Controller Designs: A Comparison Example", *in Perspectives in Control: Theory and Applications*, Dorothee Normand-Cyrot (Ed.), Springer, pp. 97-115, 1998.

3 Fittro, R. L., *A High Speed Machining Spindle with Active Magnetic Bearings: Control Theory, Design, and Application*, Ph.D dissertation, University of Virginia, 1998.

4 Namerikawa, T., Fujita, M., Matsumura, F., "Uncertainty Structure and μ-Design of a Magnetic Suspension System," *Proceedings of the Sixth International Symposium on Magnetic Bearings*, Cambridge, Mass., 1998.

5 Lindlau, J.D., *Dynamic Force Biasing of Active Magnetic Bearings Via Feedback Linearization*, MS Thesis, University of Virginia, 1999.